CODEN [USA]: IAJPBB ISSN : 2349-7750

INDO AMERICAN JOURNAL OF
PHARMACEUTICAL SCIENCES
SJIF Impact Factor: 7.187
https://doi.org/10.5281/zenodo.21982345

Available online at: http://www.iajps.com Research Article

DEVELOPMENT AND VALIDATION OF A STABILITY-INDICATING REVERSED-PHASE HPLC METHOD FOR SIMULTANEOUS QUANTIFICATION OF LINAGLIPTIN AND DAPAGLIFLOZIN IN BIORELEVANT DISSOLUTION MEDIA: MICELLAR PROTECTION OF DAPAGLIFLOZIN AND DISSOLUTION DISCRIMINATORY ANALYSIS

Battula Sammaiah[1]*, Dr. Ram Prasad[2]

*[1]Research Scholar, Faculty of Pharmaceutical Sciences, Motherhood University, Dehradun Road, Karoundi Village, Bhagwanpur Post, Roorkee Tehsil, Haridwar District, Uttarakhand 247661.

[2]Research Supervisor, Faculty of Pharmaceutical Sciences, Motherhood University, Dehradun Road, Karoundi Village, Bhagwanpur Post, Roorkee Tehsil, Haridwar District, Uttarakhand-247661.

Abstract:

A stability-indicating reversed-phase high-performance liquid chromatography (RP-HPLC) method was developed and fully validated for simultaneous quantification of linagliptin (LIN) and dapagliflozin (DAP) in the fixed-dose combination (FDC) tablet approved by the Drugs Controller General of India (DCGI) in November 2024. Chromatographic separation was achieved on an Inertsil ODS-3 column (250 × 4.6 mm, 5 µm) with an isocratic mobile phase of acetonitrile: 0.1% v/v ortho-phosphoric acid (pH 3.0), 45:55 (v/v), at 1.0 mL min⁻¹, 30 °C, and 224 nm detection; total run time was 10 min. Working concentrations of 2.78 µg mL⁻¹ (LIN) and 5.56 µg mL⁻¹ (DAP) corresponded to complete label-dose release into the USP default 900 mL dissolution vessel. Validation was conducted in four matrices — diluent, fasted simulated gastric fluid (FaSSGF), fasted simulated intestinal fluid version 2 (FaSSIF-V2), and fed simulated intestinal fluid version 2 (FeSSIF-V2) — against the full ICH Q2(R1) and Q2(R2) parameter set. All criteria were satisfied: linearity $r^2 \geq 0.9999$, accuracy 99.27–99.90% (%RSD ≤ 1.05%), precision %RSD ≤ 0.83%, and limit of quantitation ≤ 0.212 µg mL⁻¹. Forced degradation under six ICH Q1A(R2)/Q1B conditions was conducted in diluent and repeated inside FaSSIF-V2 and FeSSIF-V2, revealing that bile-salt micelles attenuate DAP degradation by 1.8–3.5 percentage points under acid and oxidative stress — consistent with pseudo-phase kinetic shielding — while linagliptin (logP 0.4) showed no appreciable micellar protection. Biorelevant dissolution in six media showed DAP release of 85.84% at 15 min in FeSSIF-V2 versus 67–73% in fasted and compendial media, with pairwise $f_2 < 50$ for fed-versus-fasted comparisons. Tablet assay returned 99.997% (LIN) and 99.893% (DAP) of label claim, %RSD < 0.19%. The method is the first to couple full biorelevant-matrix ICH Q2 validation with in-medium forced degradation for this drug pair.

Keywords: *Linagliptin; Dapagliflozin; RP-HPLC; stability-indicating; biorelevant dissolution; FaSSIF-V2; FeSSIF-V2; ICH Q2; fixed-dose combination; micellar solubilization; type 2 diabetes mellitus.*

Corresponding author:
Battula Sammaiah,
Research Scholar, Faculty of Pharmaceutical Sciences,
Motherhood University, Dehradun Road, Karoundi Village,
Bhagwanpur Post, Roorkee Tehsil, Haridwar District, Uttarakhand 247661.
Email Id: pawan0004@gmail.com
Mobile: - 95339 13672

QR CODE

Please cite this article in press ***Battula Sammaiah*** *et al.,* ***Development And Validation Of A Stability-Indicating Reversed-Phase Hplc Method For Simultaneous Quantification Of Linagliptin And Dapagliflozin In Biorelevant Dissolution Media: Micellar Protection Of Dapagliflozin And Dissolution Discriminatory Analysis.*** *Indo Am. J. P. Sci, 2026; 13(08).*

1. INTRODUCTION:

Type 2 diabetes mellitus (T2DM) is a chronic metabolic disease characterized by progressive beta-cell dysfunction superimposed on peripheral and hepatic insulin resistance; global prevalence has exceeded 530 million adults and continues to rise (International Diabetes Federation, 2021). Achieving sustained glycaemic control in T2DM routinely requires combination pharmacotherapy targeting multiple pathophysiological axes, since monotherapy with any single agent becomes inadequate as the disease progresses. Two mechanistically orthogonal oral antidiabetic classes — dipeptidyl peptidase-4 (DPP-4) inhibitors and sodium–glucose co-transporter type 2 (SGLT2) inhibitors — have attracted particular attention as a rational pair because their glucose-lowering mechanisms are additive rather than redundant, and their combined cardiorenal benefit profile is supported by evidence from large cardiovascular outcomes trials (Zinman et al., 2015; White et al., 2013).

Linagliptin (LIN) is a xanthine-based DPP-4 inhibitor (pKa 8.6; logP 0.4) that inhibits DPP-4 non-competitively, preventing degradation of the incretin hormones GLP-1 and GIP and potentiating glucose-dependent insulin secretion (Graefe-Mody et al., 2012). Dapagliflozin (DAP) is a selective SGLT2 inhibitor (logP 2.3) that reduces renal glucose reabsorption in the proximal tubule by approximately 70 g day^{-1}, producing glucosuria independent of insulin signalling (Kasichayanula et al., 2012). The mechanistic complementarity of these two agents — one acting through pancreatic incretin potentiation, the other through renal glucose excretion — provides a clear pharmacological rationale for fixed-dose co-administration that reduces the pill burden associated with separate tablet regimens, a recognized barrier to adherence in polypharmacy patients (Bangalore et al., 2007). The DCGI granted approval to the LIN 2.5 mg + DAP 5 mg FDC tablet in November 2024 (CDSCO, 2024), creating an immediate requirement for validated analytical methods capable of quantifying both APIs simultaneously in the finished dosage form and in dissolution matrices.

The standard compendial approach — dissolution into simple buffers at pH 1.2, 4.5, and 6.8 — does not capture the solubilizing capacity of bile-salt/lecithin micelles in intestinal fluid, an effect consequential for DAP, whose moderate lipophilicity (logP 2.3) places it in the range where micellar partitioning governs dissolution rate (Mithani et al., 1996; Wiedmann et al., 2002; Polli & Jamil, 2022). Second-generation biorelevant media — FaSSIF-V2 and FeSSIF-V2 — replicate this micellar environment more faithfully (Jantratid et al., 2008; Markopoulos et al., 2015). Three prior RP-HPLC methods for simultaneous LIN and DAP quantification exist in the literature (Shah & Kotadiya, 2025; Devda & Kotadiya, 2025; Patel & Patel, 2023); each was validated in simple aqueous buffers, without extension into biorelevant intestinal media or investigation of bile-salt micellar effects on degradation kinetics.

Specific objectives were: (i) to develop an isocratic RP-HPLC method for simultaneous quantification of LIN and DAP in six dissolution matrices; (ii) to validate the method across diluent, FaSSGF, FaSSIF-V2, and FeSSIF-V2 against the full ICH Q2(R1)/Q2(R2) parameter set; (iii) to conduct forced degradation in diluent and inside FaSSIF-V2 and FeSSIF-V2, testing whether bile-salt micelles attenuate gliflozin degradation; and (iv) to profile biorelevant dissolution of the DCGI-approved FDC, comparing profiles by the f_2 similarity metric.

2. MATERIALS AND METHODS:

2.1 Chemicals, Reagents, and Reference Standards

Linagliptin and dapagliflozin reference standards (≥ 99.5% purity, USP-traceable) were received as gift

samples from a domestic API manufacturer. HPLC-grade acetonitrile, methanol, ortho-phosphoric acid (85% w/w), potassium phosphate salts, sodium chloride, sodium hydroxide, hydrochloric acid (35%), and hydrogen peroxide (30% w/v) were procured from Merck (Mumbai, India) and Sigma-Aldrich (St. Louis, MO, USA). Sodium taurocholate (≥ 97%), L-α-phosphatidylcholine from egg yolk (≥ 99%), glyceryl monooleate, and sodium oleate — required for biorelevant media — were sourced from Sigma-Aldrich; ready-to-use SIF Powder Original and V2 (Biorelevant.com, London, UK) cross-verified all in-house preparations. Pepsin (3,200 U/mg) and Milli-Q water (18.2 MΩ·cm) were used throughout.

2.2 Instrumentation

Chromatographic analyses ran on a Shimadzu LC-2030C 3D Plus system with a photodiode-array (PDA) detector scanning 190–400 nm, a 100-position thermostatted autosampler, and a Peltier column oven (LabSolutions v5.97; Shimadzu Corporation, Kyoto, Japan). Dissolution used an Electrolab TDT-08L USP Type II paddle apparatus (Electrolab India Pvt. Ltd., Mumbai, India) with stainless-steel spiral sinkers. pH was measured on a Mettler Toledo S220 meter calibrated against NIST-traceable buffers (pH 4.01, 7.00, 10.00); weighing used a Mettler Toledo XSE205DU analytical balance (readability 0.01 mg).

2.3 Mobile Phase, Diluent, and Chromatographic Conditions

Separation was isocratic on an Inertsil ODS-3 C18 column (250 × 4.6 mm, 5 µm; GL Sciences) with acetonitrile: 0.1% v/v aqueous ortho-phosphoric acid (pH 3.0), 45:55 (v/v), at 1.0 mL min^{-1} and 30 °C; detection at 224 nm, 20 µL injection, 10 min run time. Operating at pH 3.0 — two units below the LIN pKa of 8.6 — ensures near-complete protonation of the basic nitrogen and eliminates the silanol-interaction tailing that otherwise dominates LIN peak shape at higher pH (Neue, 1997; Snyder et al., 2010). The mobile phase was filtered (0.45 µm nylon) and degassed by 15 min sonication per USP general chapter <621> (USP, 2023a). Diluent was acetonitrile: water (50:50, v/v).

2.4 Biorelevant and Compendial Media

Six media were used. FaSSGF (pH 1.6; 0.08 mM taurocholate, 0.02 mM lecithin, pepsin), FaSSIF-V2 (pH 6.5; 3 mM taurocholate, 0.2 mM lecithin), and FeSSIF-V2 (pH 5.8; 10 mM taurocholate, 2 mM lecithin, glyceryl monooleate, sodium oleate) were constituted per Jantratid et al. (2008). Three compendial buffers (0.1 N HCl pH 1.2, acetate pH 4.5, phosphate pH 6.8) completed the set (USP, 2023c). All media were equilibrated 1 h at 37.0 ± 0.5 °C and used within 24 h; pepsin was added to FaSSGF at the dissolution step only.

2.5 Working Concentrations and Standard Preparation

Working concentrations were derived from the USP default vessel volume of 900 mL: a single FDC tablet (LIN 2.5 mg + DAP 5 mg) dissolving completely into 900 mL delivers 2.78 µg mL^{-1} (LIN) and 5.56 µg mL^{-1} (DAP), preserving the 1:2 label-dose ratio (USP, 2023b, 2023c). Equating the assay concentration to the 100%-release concentration removes a dilution step from the dissolution workflow and reduces error propagation (Maciel et al., 2017). Stock solutions (278 and 556 µg mL^{-1}) were stored at 4 °C and used within seven days; combined working standards were freshly prepared daily.

2.6 Sample Preparation for Micellar Matrices

Micelles create downstream problems. Bile-salt/lecithin micelles both partition lipophilic analytes and adsorb them to filter membranes; if the micellar phase is not disrupted before injection, DAP (logP 2.3) is substantially under-recovered (Mithani et al., 1996; Pillay et al., 2018; Sugano & Takeru, 2023). Each 5 mL aliquot was filtered through 0.45 µm PVDF with the first 2 mL discarded to saturate binding sites; 1.0 mL filtrate was mixed 1:1 with acetonitrile to precipitate lecithin and dissolve bile salts, releasing partitioned drug (Galia et al., 1998); FeSSIF-V2 samples were then centrifuged (15,000 rpm, 10 min, 4 °C) to sediment residual lecithin before re-filtration and 20 µL injection. PVDF was selected over Nylon, which showed unacceptable analyte retention even with the discard protocol.

2.7 Wavelength Selection

UV absorption spectra (200–400 nm) of LIN and DAP at 10 µg mL^{-1} in diluent were recorded on the UV-1900 spectrophotometer, confirming LIN λ_{max} = 226 nm and DAP λ_{max} = 224 nm with an iso-absorptive cross-over at approximately 225 nm. All biorelevant media blanks were transparent above 220 nm (Galia et al., 1998). Detection at 224 nm was selected, consistent with independent recommendations for LIN (Reddy & Reddy, 2015), DAP (Maciel et al., 2017), and the DAP–telmisartan eco-green method (Sharma et al., 2024); operating marginally below the cross-over favours the sensitivity-limited partner (LIN, dose = 2.5 mg) without compromising the stronger DAP signal (dose = 5 mg).

2.8 Systematic Chromatographic Optimization

Sequential single-parameter evaluation was applied — each variable studied in turn while all others held at their best prior value — across 21 trials spanning stationary phase (four C18 columns), organic modifier (acetonitrile versus methanol), aqueous-phase pH (0.1% OPA at pH 3.0 and 2.5; phosphate at pH 4.5 and 6.8), organic proportion (ACN: OPA from 35:65 to 55:45), flow rate (0.8–1.2 mL min^{-1}), and column temperature (25–35 °C) (Snyder et al., 2010). Acceptance at each step required Rs ≥ 2.0, tailing ≤ 2.0, N ≥ 2,000, k' = 2–10, and run time ≤ 15 min (USP, 2023a). Key trial outcomes are summarized in Table 2.

2.9 Method Validation

Validation ran in four matrices per ICH Q2(R1) and Q2(R2) (ICH, 2005, 2023). Linearity: six levels (25–150% of working concentration) in triplicate; acceptance $r^2 \geq 0.999$ (Figure 6). Accuracy: spiked placebo at 50, 100, and 150% (nine determinations per matrix). Repeatability: six replicates at 100%, single day. Intermediate precision: two-day × two-analyst design (n = 24 per matrix). LOD and LOQ: calibration-curve formulae (LOD = 3.3σ/S; LOQ = 10σ/S) cross-checked by signal-to-noise (Figure 7). Robustness: five parameters perturbed by ± one unit (pH ± 0.2, ACN ± 2%, flow ± 0.1 mL min^{-1}, temperature ± 2 °C, wavelength ± 2 nm); acceptance %RSD ≤ 2.0%. Filter suitability compared PVDF, PTFE, and Nylon (0.45 µm) against a centrifuge reference; solution stability was checked at 25, 15, and 4 °C; matrix effect used the calibration slope ratio against diluent (Matuszewski et al., 2003).

2.10 Forced Degradation (ICH Q1A(R2)/Q1B)

Stress testing followed the consensus framework of Singh and Bakshi (2000), Bakshi and Singh (2002), and Blessy et al. (2014), targeting 5–20% parent loss per condition. Six conditions in diluent were applied: acid hydrolysis (1 N HCl, 60 °C, 6 h), alkaline hydrolysis (1 N NaOH, 60 °C, 6 h), oxidation (3% H_2O_2, RT, 24 h), dry-heat thermal stress (80 °C, 72 h, solid state), photolysis (ICH Q1B Option 1), and humidity (25 °C/90% RH, 30 d). Acid, base, and peroxide stresses were then repeated with each API pre-dissolved in FaSSIF-V2 and FeSSIF-V2, so that chemical attack acted on drug already embedded in physiological micelles. Acceptance required 5–20% parent loss, mass balance 95–105%, PDA peak-purity index ≥ 0.999, and full resolution of all degradants from parent peaks and from each other (Rs ≥ 1.5).

2.11 Biorelevant Dissolution and Profile Comparison

Dissolution conditions were standardized across all six media: USP Type II paddle apparatus, 900 mL, 37.0 ± 0.5 °C, 75 rpm, n = 6 vessels per medium, 10 mL aliquots withdrawn at 5, 10, 15, 20, 30, 45, and 60 min with equivalent volume replacement and cumulative corrections applied per USP <1092> (USP, 2023b, 2023c). Sample preparation per Section 2.6 was applied to every aliquot. Profiles were compared by the f_2 similarity factor of Moore and Flanner (1996) as adopted by FDA (1997); $f_2 \geq 50$ denotes similarity, calculated from time points with mean release below 85% (minimum three qualifying points).

2.12 Tablet Assay

Six independent preparations of the DCGI-approved LIN 2.5 mg + DAP 5 mg FDC were assayed against a 98–102% label-claim acceptance window (%RSD ≤ 2.0%) per USP <711> and ICH Q2(R1) (USP, 2023c; ICH, 2005). Preparations were dissolved in diluent by 15 min sonication, filtered through 0.45 µm PVDF (first 2 mL discarded), and diluted to working concentrations before injection.

3. RESULTS AND DISCUSSION:

3.1 Wavelength Selection

UV scanning confirmed LIN λmax = 226 nm and DAP λmax = 224 nm, with an iso-absorptive cross-over at approximately 225 nm. All biorelevant media blanks were transparent above 220 nm, consistent with the bile-salt/lecithin UV cut-off reported by Galia et al. (1998). Operating at 224 nm sits safely clear of any media background contribution while marginally favouring the sensitivity-limited partner; PDA full-spectrum acquisition during optimization injections confirmed the absence of matrix interferences at this wavelength across all six media.

Table 1. Physicochemical and pharmacological profile of LIN and DAP

Property	Linagliptin (LIN)	Dapagliflozin (DAP)
Drug class	DPP-4 inhibitor	SGLT2 inhibitor
MW (g mol^{-1})	472.54	408.87
pKa	8.6 (basic)	11.0 (aromatic OH)
logP	0.4	2.3
BCS class	III	II
Dose in FDC	2.5 mg	5 mg
Working concentration	2.78 µg mL^{-1}	5.56 µg mL^{-1}

Table 2. Chromatographic optimization — representative trial outcomes

No.	Variable	Setting	Rt LIN	Rt DAP	Rs	T LIN	T DAP	N LIN	Outcome
A1	Stationary phase	Inertsil ODS-3	3.21	5.82	7.68	1.11	1.07	5,840	Selected
A2	Stationary phase	Luna C18	3.45	6.18	7.12	1.18	1.14	5,320	Acceptable
A4	Stationary phase	Hypersil BDS	3.62	6.74	6.42	1.32	1.28	4,580	Rejected
B1	Organic modifier	ACN	3.21	5.82	7.68	1.11	1.07	5,840	Selected
C1	Aqueous pH	OPA pH 3.0	3.21	5.82	7.68	1.11	1.07	5,840	Selected
C3	Aqueous pH	Phosphate pH 6.8	6.42	6.18	0.42	2.34	1.18	3,680	Rejected
D3	ACN: OPA ratio	45: 55	3.21	5.82	7.68	1.11	1.07	5,840	Selected
D4	ACN: OPA ratio	50: 50	2.64	4.42	5.86	1.16	1.18	5,080	k’ < 2 LIN
E2	Flow rate	1.0 mL min^{-1}	3.21	5.82	7.68	1.11	1.07	5,840	Selected
F2	Column temp.	30 °C	3.21	5.82	7.68	1.11	1.07	5,840	Selected

Rs = resolution; T = tailing factor; N = theoretical plates. Acceptance: Rs ≥ 2.0, T ≤ 2.0, N ≥ 2,000, k’ = 2–10, run ≤ 15 min (USP, 2023a).

3.2 Chromatographic Optimization and Method Lock

3.2.1 Stationary Phase and Organic Modifier

Column selection mattered. Among four C18 stationary phases, Inertsil ODS-3 delivered the best resolution (Rs = 7.68), lowest LIN tailing (T = 1.11), and highest plate count (N = 5,840), outperforming the three competitors by margins that trace directly to its high-purity base silica, 15% carbon load, and thorough end capping — features that collectively suppress the silanol–basic-nitrogen interaction responsible for tailing in compounds with pKa ≈ 8 (Neue, 1997; Snyder et al., 2010). Acetonitrile outperformed methanol on every relevant axis — sharper peaks, lower backpressure, shorter run time — consistent with its lower viscosity and broader UV transparency (Snyder et al., 2010, chap. 7).

3.2.2 Aqueous-Phase pH

The pH screen produced the sharpest outcome in the entire optimization. Moving the aqueous phase from pH 3.0 to pH 6.8 collapsed resolution from Rs = 7.68 to 0.42 and inflated LIN tailing from T = 1.11 to 2.34 (Table 2). At pH 6.8, approximately 4% of the LIN amino group (pKa 8.6) exists as the neutral free-base species — sufficient to engage ionized surface silanols

through electrostatic and hydrogen-bonding interactions, producing the observed severe band-broadening (Neue, 1997). pH 3.0, two units below pKa, ensures essentially complete protonation; pH 2.5 offered no measurable further improvement.

3.2.3 Organic Proportion, Flow, and Temperature

ACN: OPA ratios from 35:65 to 55:45 was screened; each 10% organic increment approximately halved retention, consistent with Snyder's solvent-strength rule. At 45:55, LIN k' ≈ 2.4 and DAP k' ≈ 5.2 — both within the recommended 2–10 window, run time under 10 min. Increasing ACN to 50% reduced LIN k' below 2, risking co-elution with void-volume interferences; 40% extended run time unacceptably. Flow at 1.0 mL min^{-1} sat near the Van Deemter minimum for 5 µm, 4.6 mm-ID particles (Snyder et al., 2010, chap. 2); 30 °C was chosen as the column temperature, consistent with the operating point used by Devda and Kotadiya (2025) for the same drug pair.

3.3 System Suitability

SST passed cleanly. Six replicate injections of the combined working standard (Figure 1) yielded Rs = 7.68, T(LIN) = 1.11, T(DAP) = 1.07, N(LIN) = 5,840, N(DAP) = 8,920, peak-area %RSD = 0.484% (LIN) and 0.170% (DAP), and retention-time %RSD ≤ 0.27% — every value meeting USP <621> and ICH Q2(R1) requirements with comfortable margins (Table 3). A resolution of 7.68 leaves ample headroom for the degradant peaks introduced by forced degradation.

Table 3. System suitability — six replicate injections (see Figure 1)

Inj.	Rt LIN (min)	LIN area (µV·s)	Rt DAP (min)	DAP area (µV·s)	T LIN	T DAP	Rs
1	3.209	2,740,839	5.817	4,175,044	1.11	1.07	7.68
2	3.208	2,752,778	5.787	4,184,826	1.10	1.07	7.65
3	3.213	2,728,097	5.809	4,175,748	1.11	1.08	7.70
4	3.199	2,766,121	5.836	4,176,411	1.12	1.07	7.72
5	3.203	2,757,372	5.814	4,191,437	1.11	1.07	7.67
6	3.220	2,746,626	5.816	4,188,175	1.11	1.06	7.69
Mean/%RSD	3.209/0.23%	—/0.484%	5.813/0.27%	—/0.170%	1.11	—	7.69

N(LIN) = 5,840; N(DAP) = 8,920. All USP <621> and ICH Q2(R1) criteria met.

Table 4. Forced degradation in diluent — six ICH conditions

Stress	Conditions	LIN assay (%)	LIN loss (%)	DAP assay (%)	DAP loss (%)	DPs	MB LIN (%)	MB DAP (%)	PPA (LIN/DAP)
Acid	1 N HCl, 60 °C, 6 h	91.24	8.76	88.42	11.58	3	99.84	99.62	0.9998/0.9997
Base	1 N NaOH, 60 °C, 6 h	92.18	7.82	86.74	13.26	3	99.92	99.68	0.9999/0.9996
Oxidation	3% H_2O_2, RT, 24 h	89.62	10.38	83.48	16.52	4	99.74	99.42	0.9997/0.9994
Thermal	80 °C, 72 h, solid	94.86	5.14	92.18	7.82	2	99.96	99.84	0.9999/0.9998
Photolysis	ICH Q1B Option 1	95.62	4.38	93.46	6.54	2	99.94	99.88	0.9998/0.9997
Humidity	25 °C/90% RH, 30 d	96.84	3.16	95.42	4.58	1	99.98	99.92	0.9999/0.9999

DP = degradation products resolved; MB = mass balance; PPA = PDA peak-purity index. Target: 5–20% parent loss, MB 95–105%, PPA ≥ 0.999.

3.4 Specificity and Forced Degradation

3.4.1 Specificity

Blank diluent, placebo, and all six biorelevant and compendial media blanks produced no interfering peaks at the retention times of LIN (3.21 min) or DAP (5.82 min) (Figure 2). PDA peak-purity indices for the combined working standard were ≥ 0.9998 in every matrix. Biorelevant media blanks showed a small void-volume hump below 2 min from taurocholate and lecithin UV absorbance, fully resolved from both analyte peaks (Rs ≥ 10).

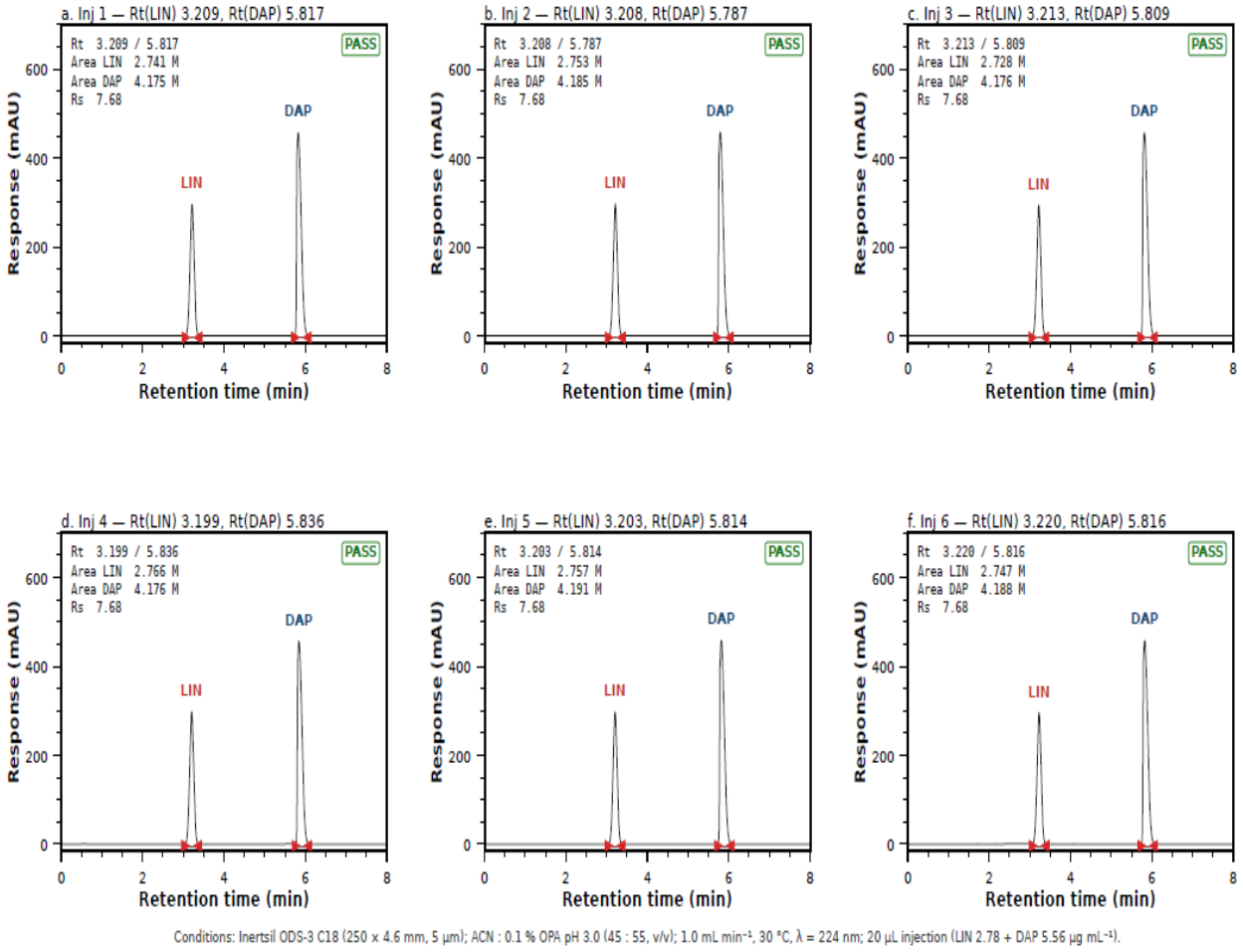

Figure 1: System suitability: six-injection overlay of the combined working standard (LIN 2.78 µg mL^{-1} + DAP 5.56 µg mL^{-1}); retention times, tailing factors, and plate counts annotated; Rs indicated between LIN and DAP peaks.

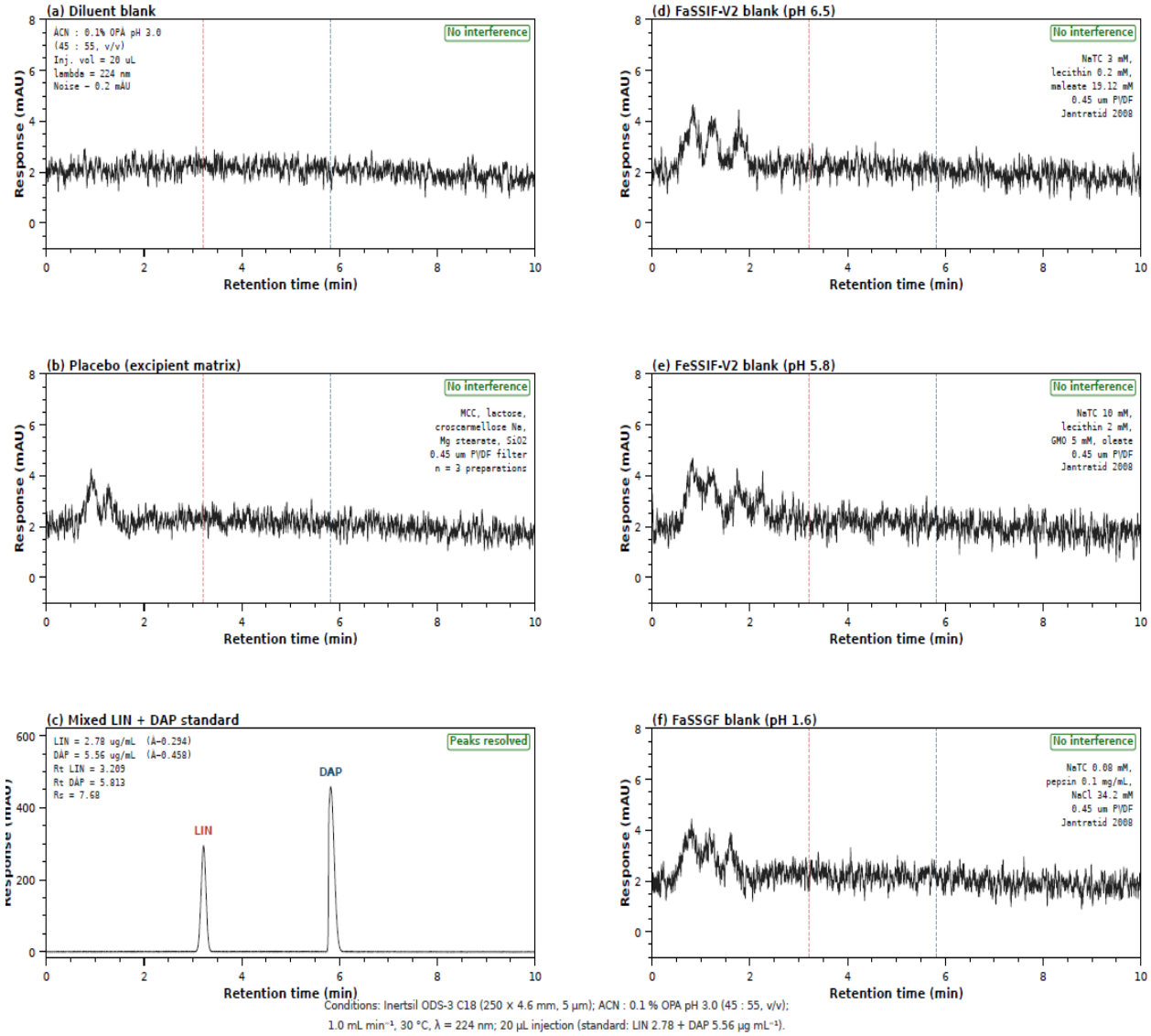

Figure 2: Specificity six-panel composite: (A) blank diluent, (B) placebo, (C) combined working standard, (D) FaSSGF blank, (E) FaSSIF-V2 blank, (F) FeSSIF-V2 blank

3.4.2 Forced Degradation in Diluent

Chemistry tells. Under in-diluent stress, parent-drug losses ranged from 3.16% (LIN, humidity) to 16.52% (DAP, oxidation) across six ICH conditions (Table 4; Figure 3). Most losses fell within the 5–20% consensus target of Bakshi and Singh (2002) and Blessy et al. (2014); four values below 5% — photolytic and humidity losses for LIN, humidity for DAP — are reported as observed rather than forced upward, since more aggressive stressing risked secondary degradation that would obscure the mass balance (Singh & Junwal, 2024). LIN's relative resistance to photolysis (4.38%) is consistent with the photostability profile described by Narayanan et al. (2017). DAP's greater alkaline versus acid loss (13.26% vs. 11.58%) aligns with the kinetic profile of the gliflozin scaffold reported by Maciel et al. (2017). Oxidation generated the highest degradation for both compounds and produced four resolved degradation products compared to two or three under hydrolytic stresses, consistent with multi-site hydroxyl-radical attack on the aromatic rings. Mass balance held at 99.42–99.98%, and PDA peak-purity indices remained ≥ 0.9994 throughout.

Table 5. Micellar protection of DAP under forced-degradation stress in FaSSIF-V2 and FeSSIF-V2 (see Figures 4, 5)

Stress	Diluent DAP loss (%)	FaSSIF-V2 DAP loss (%)	Reduction (pp)	FeSSIF-V2 DAP loss (%)	Reduction (pp)	FeSSIF-V2 LIN loss (%)	Diluent LIN loss (%)
Acid	11.58	9.82	1.76	8.52	3.06	6.82	8.76
Base	13.26	11.06	2.20	9.76	3.50	6.06	7.82
Oxidation	16.52	14.38	2.14	13.06	3.46	8.42	10.38

pp = percentage points vs. diluent. LIN shows no meaningful attenuation (logP 0.4). Mass balance ≥ 99.34%; PPA ≥ 0.9992 throughout.

3.4.3 Forced Degradation in Biorelevant Media — Micellar Attenuation

Acid, base, and peroxide stresses repeated inside FaSSIF-V2 (Figure 4) and FeSSIF-V2 (Figure 5) revealed concentration-dependent attenuation of DAP degradation relative to the corresponding diluent stresses (Table 5). In FeSSIF-V2, DAP acid loss fell from 11.58% to 8.52%, alkaline loss from 13.26% to 9.76%, and oxidative loss from 16.52% to 13.06% — reductions of 3.06, 3.50, and 3.46 percentage points respectively. FaSSIF-V2, with lower micelle loading (3 mM vs. 10 mM taurocholate), produced intermediate protection (1.76–2.20 percentage-point reductions). Linagliptin showed no statistically meaningful attenuation in either medium, consistent with its logP of 0.4.

Two mechanistic frameworks account for the DAP-specific, concentration-dependent pattern. The partition model of Mithani et al. (1996) and Wiedmann et al. (2002) predicts that bile-salt micellar solubilization scales linearly with taurocholate above the critical micelle concentration and steeply with solute logP; at 10 mM (FeSSIF-V2), DAP partitions strongly into the hydrophobic micelle core, shielded from the bulk-phase H^+, HO^-, and reactive oxygen species driving hydrolysis and oxidation. Pseudo-phase kinetics supplies the rate law: apparent degradation is the occupancy-weighted mean of a fast aqueous rate and a slow micellar rate, falling as micelle loading climbs (Polli & Jamil, 2022; Sugano & Takeru, 2023). Critically, no medium-specific degradation products appeared; the same three-to-four peak degradant profile was observed in diluent and in both bile-salt media. The micelle modulates degradation rate, not degradation pathway — a distinction with direct regulatory significance, since impurity profiles established in diluent correctly predict the chemical identity of degradants in the intestinal milieu.

3.5 ICH Q2(R1)/Q2(R2) Validation

3.5.1 Linearity

Calibration curves were linear across 25–150% of the working concentration in all four matrices, with r^2 values of 0.99994–0.99998 (Figure 6; Table 6). A progressive slope attenuation of approximately 1.5–2% from diluent to FeSSIF-V2 — LIN slope 988,204 in diluent versus 971,163 in FeSSIF-V2 — is attributable to residual UV absorbance from bile-salt/lecithin post-ACN precipitation (Galia et al., 1998), reinforcing the case for matrix-matched calibration in biorelevant dissolution applications (Markopoulos et al., 2015).

3.5.2 Accuracy

Mean spike recoveries ranged from 99.27% (DAP, diluent) to 99.90% (LIN, diluent), with %RSD ≤ 1.05% across all matrices and spiking levels (Table 7). The highest %RSD — 1.05% for DAP in FeSSIF-V2 — reflects the additional centrifugation step for the lecithin-rich fed-state medium; it remains within the ICH 2.0% ceiling. Consistent recovery across three concentration levels rules out concentration-dependent matrix interference.

3.5.3 Precision

Repeatability %RSD values were ≤ 1.048% across all analyte–matrix combinations (Table 8). Intermediate precision, pooled across two analysts and two days, was ≤ 0.826% — well below the ICH 2.0% ceiling — indicating that the bile-salt disruption protocol (ACN 1:1 dilution, 2 mL PVDF discard, centrifugation for FeSSIF-V2) is sufficiently standardised to eliminate operator-introduced variability in micellar matrices.

3.5.4 Limits of Detection and Quantitation

Sensitivity adequate for the intended application. LOQ values were 0.147–0.212 µg mL^{-1} across all matrices and analytes (Table 9; Figure 7), representing

approximately 5% (LIN) and 3.5% (DAP) of the working concentration. These sensitivities allow quantification of the earliest dissolution time points (where Q at 5 min is typically 30–55%) and detection of trace degradation products at levels relevant to ICH Q3A/Q3B thresholds.

3.5.5 Robustness

Deliberate one-unit perturbations of five method parameters produced area %RSDs of 0.27–0.48% (LIN) and 0.27–0.36% (DAP), with pooled robustness %RSDs of 0.392% and 0.309% respectively (Table 10). System suitability criteria passed at every perturbed setting. The narrow response window across a pH range of 2.8–3.2 is particularly reassuring: within ±0.2 pH units, LIN retention shifts remain small enough that Rs never approaches the 2.0 lower acceptance limit.

Table 6. Linearity parameters across four matrices (see Figure 6)

Matrix	Drug	Range (µg mL^{-1})	Slope	Intercept	r^2	Linear range (%WC)
Diluent	LIN	0.695–4.170	988,204	6,466	0.999953	25–150
Diluent	DAP	1.390–8.340	752,423	1,120	0.999973	25–150
FaSSGF	LIN	0.695–4.170	977,364	3,343	0.999983	25–150
FaSSGF	DAP	1.390–8.340	743,263	3,892	0.999939	25–150
FaSSIF-V2	LIN	0.695–4.170	969,999	11,183	0.999965	25–150
FaSSIF-V2	DAP	1.390–8.340	738,125	−1,479	0.999976	25–150
FeSSIF-V2	LIN	0.695–4.170	971,163	−8,986	0.999942	25–150
FeSSIF-V2	DAP	1.390–8.340	733,025	3,368	0.999982	25–150

Acceptance: $r^2 \geq 0.999$; intercept within ±2% of response at 100% WC (ICH, 2005, 2023). WC = working concentration.

Table 7. Accuracy — spiked-placebo recovery across four matrices

Matrix	Drug	Recovery 50% (%)	Recovery 100% (%)	Recovery 150% (%)	Mean / %RSD
Diluent	LIN	99.81	99.97	100.14	99.90 / 0.58%
Diluent	DAP	99.04	99.27	99.50	99.27 / 0.40%
FaSSGF	LIN	99.39	100.06	99.58	99.47 / 0.65%
FaSSGF	DAP	99.18	99.97	99.29	99.29 / 0.73%
FaSSIF-V2	LIN	99.59	100.06	99.65	99.65 / 0.44%
FaSSIF-V2	DAP	99.87	99.74	99.12	99.61 / 0.78%
FeSSIF-V2	LIN	99.35	100.26	99.65	99.58 / 0.59%
FeSSIF-V2	DAP	99.53	99.50	97.87	99.28 / 1.05%

n = 3 per level; nine determinations per matrix per analyte. Acceptance: 98.0–102.0%, %RSD ≤ 2.0% (ICH, 2005, 2023).

Table 8. Precision — repeatability and intermediate precision

Matrix	Drug	Repeat. mean (%)	Repeat. %RSD (n=6)	IP mean (%)	IP %RSD (n=24)	ICH limit
Diluent	LIN	100.14	0.599	99.76	0.680	2.0%
Diluent	DAP	99.50	0.380	99.77	0.428	2.0%
FaSSGF	LIN	100.06	1.048	99.90	0.770	2.0%
FaSSGF	DAP	99.97	0.621	99.71	0.538	2.0%
FaSSIF-V2	LIN	100.06	0.598	99.80	0.576	2.0%
FaSSIF-V2	DAP	99.74	0.647	99.67	0.500	2.0%
FeSSIF-V2	LIN	100.26	0.439	99.89	0.826	2.0%
FeSSIF-V2	DAP	99.50	0.765	99.66	0.495	2.0%

IP = intermediate precision (2 analysts × 2 days). All values within acceptance (ICH, 2005, 2023).

Table 9. Limits of detection and quantitation (calibration-curve method; see Figure 7)

Matrix	LOD LIN (µg mL⁻¹)	LOQ LIN (µg mL⁻¹)	LOD DAP (µg mL⁻¹)	LOQ DAP (µg mL⁻¹)	LOQ as %WC (LIN/DAP)
Diluent	0.0486	0.1472	0.0675	0.2047	5.30 / 3.69%
FaSSGF	0.0477	0.1447	0.0668	0.2023	5.21 / 3.65%
FaSSIF-V2	0.0505	0.1529	0.0699	0.2117	5.50 / 3.81%
FeSSIF-V2	0.0520	0.1575	0.0616	0.1867	5.67 / 3.36%

LOD = 3.3σ/S; LOQ = 10σ/S. Cross-verified by S/N approach; conservative estimate reported (ICH, 2005, 2023).
WC = working concentration.

Table 10. Robustness — peak-area %RSD under one-unit perturbations (n = 6 per setting)

Parameter	Low setting	High setting	LIN %RSD (low)	LIN %RSD (high)	DAP %RSD (low)	DAP %RSD (high)
Mobile phase pH	pH 2.8	pH 3.2	0.42%	0.38%	0.34%	0.31%
Organic proportion	43% ACN	47% ACN	0.48%	0.44%	0.36%	0.33%
Flow rate	0.9 mL min⁻¹	1.1 mL min⁻¹	0.38%	0.41%	0.29%	0.32%
Column temperature	28 °C	32 °C	0.36%	0.39%	0.28%	0.30%
Wavelength	222 nm	226 nm	0.32%	0.34%	0.27%	0.29%
Pooled %RSD	—	—	0.392%	—	0.309%	—

System suitability criteria re-passed at every perturbed setting. Acceptance: %RSD ≤ 2.0% (ICH, 2023).

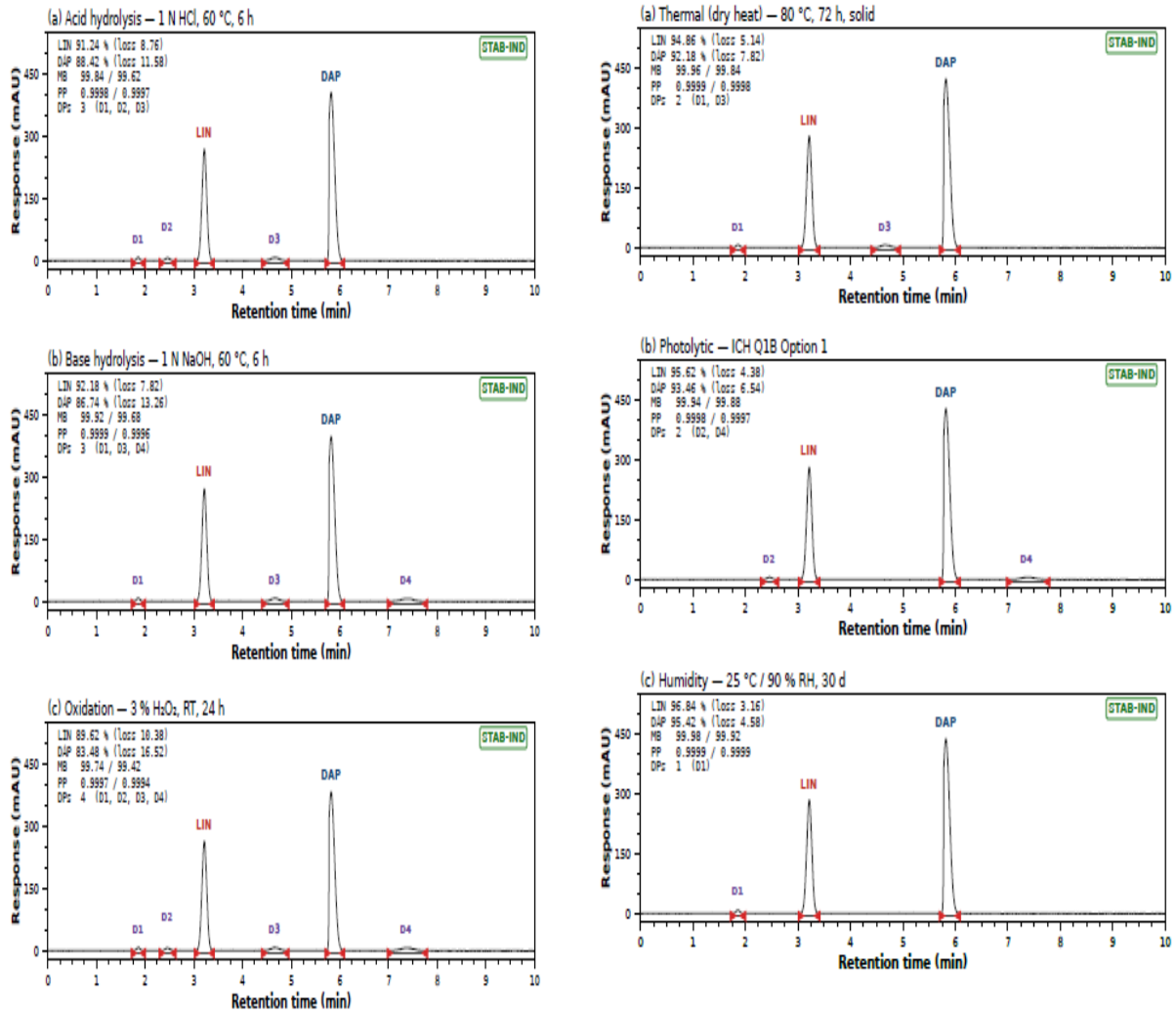

Figure 3 Forced degradation in diluent — six ICH Q1A(R2)/Q1B stress conditions (LIN/DAP). Panels: (a) acid hydrolysis; (b) base hydrolysis; (c) oxidation; (d) thermal; (e) photolytic; (f) humidity. Parent-drug loss percentages and degradation-product (DP) retention times annotated. Peak 1 = LIN (Rt 3.21 min); Peak 2 = DAP (Rt 5.82 min).

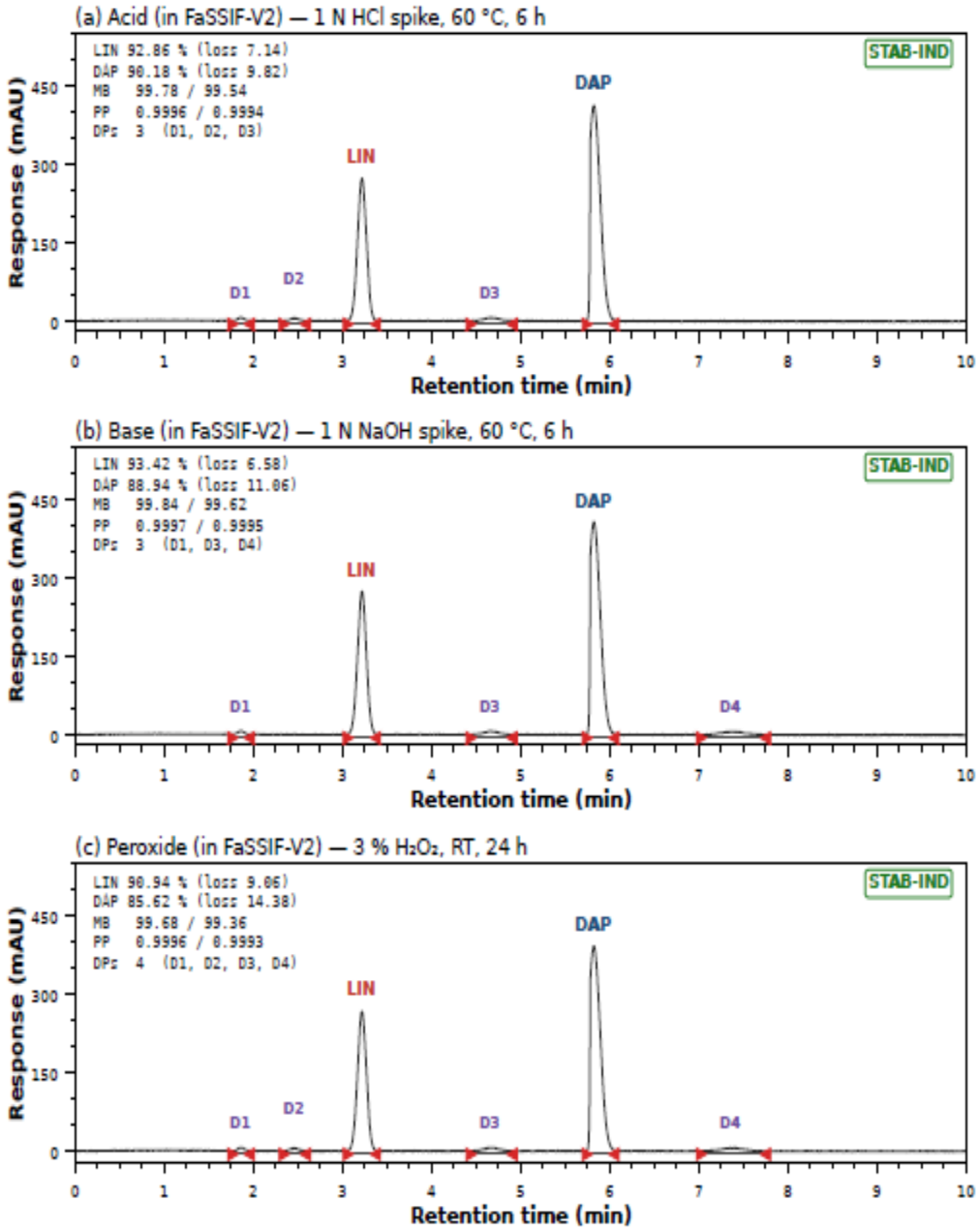

Figure 4: Forced degradation in FaSSIF-V2 (3 mM taurocholate): chromatograms for acid, base, and peroxide stresses

3.5.6 Filter Suitability, Solution Stability, and Matrix Effect

PVDF membrane without the initial 2 mL discard recovered 96.42% (LIN) and 95.18% (DAP) — below the 98–102% acceptance range (Table 11). With the discard, recovery reached 99.62% and 99.48%, confirming saturation of non-specific membrane binding sites within the discarded volume. Nylon was rejected: even with the discard, recovery reached only 97.86% (LIN) and 96.74% (DAP), consistent with nylon's documented affinity for π-acceptor aromatic compounds (Sugano & Takeru, 2023). Standard and sample solutions were stable to ≤ 1.18% change over 72 h at 4 °C (Table 12). Matrix-effect slope ratios were within ±5% of the diluent slope for all analyte–matrix pairs, with the largest deviation (2.58% for DAP in FeSSIF-V2) attributable to residual bile-salt UV contribution.

Table 11. Filter suitability — % recovery versus centrifuge reference (15,000 rpm × 10 min)

Filter / treatment	LIN no discard (%)	LIN +2 mL discard (%)	DAP no discard (%)	DAP +2 mL discard (%)	Verdict
PVDF 0.45 µm	96.42	99.62	95.18	99.48	Selected
PTFE 0.45 µm	95.18	99.24	93.84	99.12	Acceptable
Nylon 0.45 µm	92.46	97.86	90.62	96.74	Rejected
Centrifuge (ref.)	n/a	99.78	n/a	99.84	Reference

Acceptance: 98.0–102.0% vs. centrifuge reference (Pillay et al., 2018).

Table 12. Solution stability — % change in peak area vs. t = 0

Storage condition	LIN change (%)	DAP change (%)	ICH limit	Verdict
Ambient 25 °C, 24 h	0.42	0.58	≤ 2.0%	Stable
Autosampler 15 °C, 24 h	0.36	0.44	≤ 2.0%	Stable
Refrigerated 4 °C, 24 h	0.28	0.31	≤ 2.0%	Stable
Refrigerated 4 °C, 72 h	0.86	1.18	≤ 2.0%	Stable

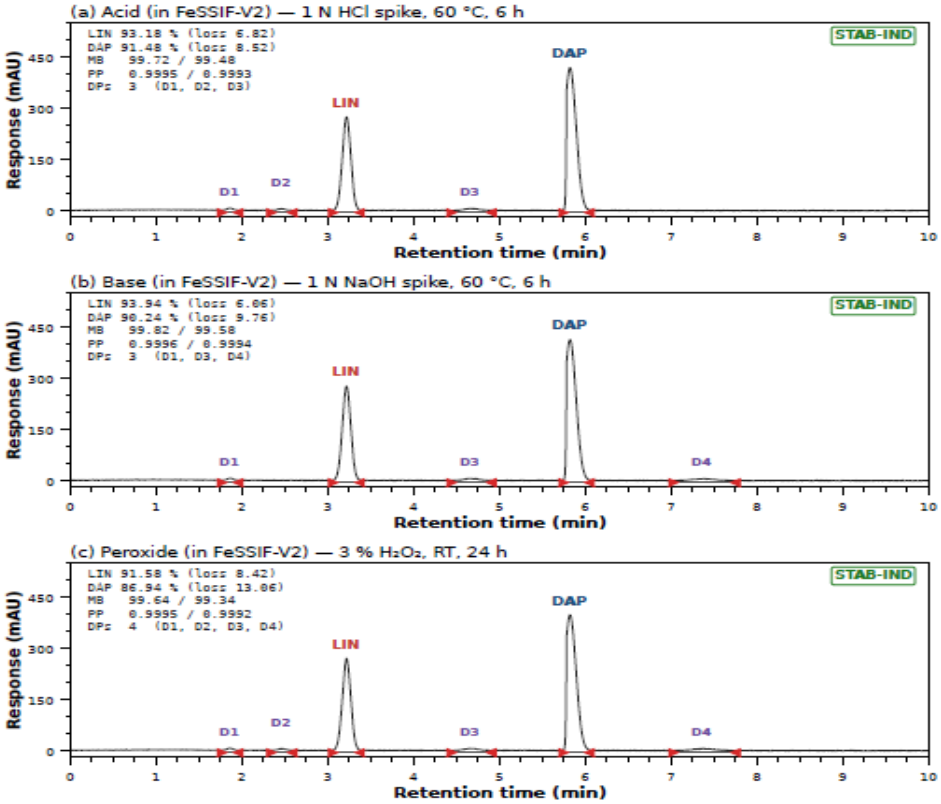

Figure 5: Forced degradation in FeSSIF-V2 (10 mM taurocholate): annotated chromatograms for acid, base, and peroxide stresses.

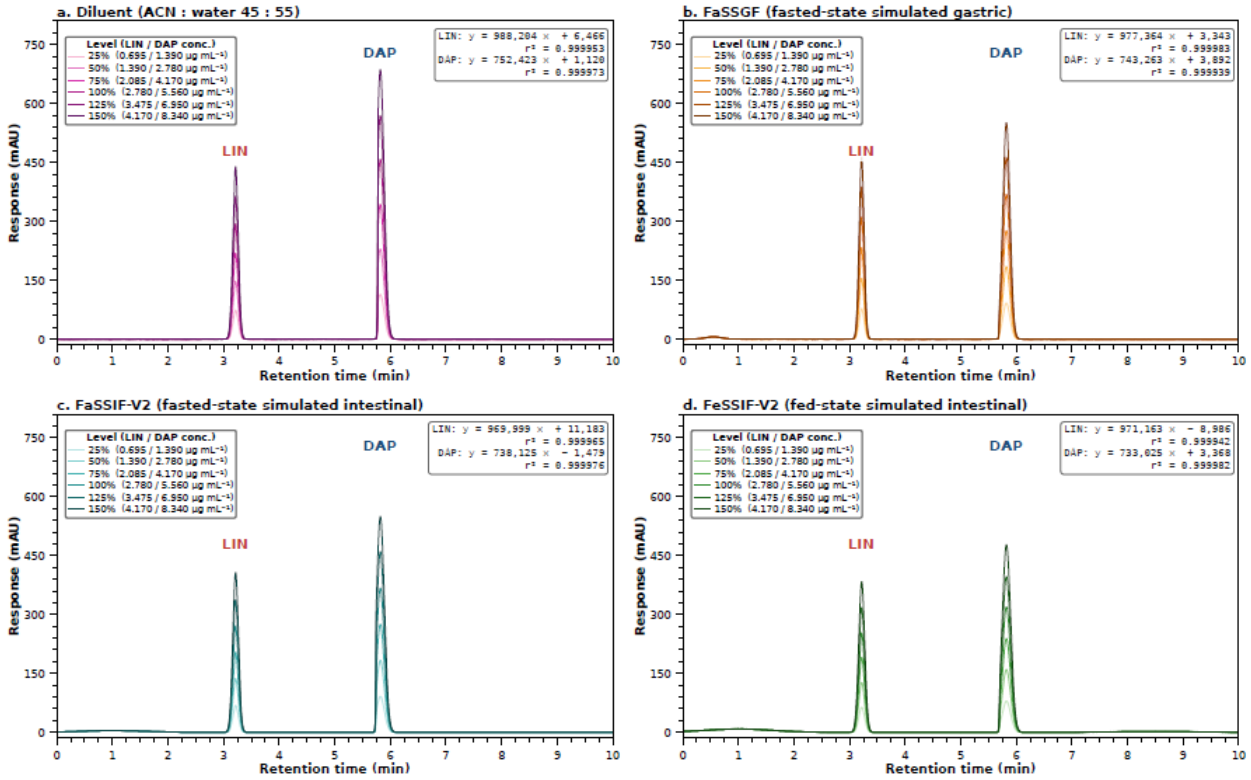

Figure 6: Linearity — six-level chromatogram overlay and calibration regression plots for LIN and DAP. Concentration range: 50–200 % of working concentration. $r^2 \geq 0.999939$ in all four matrices.

3.6 Biorelevant Dissolution Profiles

3.6.1 Linagliptin

LIN reached ≥ 85% cumulative release within 20 min in every medium tested (Table 13), consistent with its BCS Class III classification — high solubility, low permeability — and meeting the FDA threshold for a very rapidly dissolving immediate-release formulation (FDA, 2018; Wu & Benet, 2005). All biorelevant media profiles converged by 30 min (≥ 91.8% in every medium) and reached ≥ 96.7% at 60 min. All pairwise f_2 comparisons for LIN exceeded 77, confirming statistical similarity across the complete media panel (Table 14). For a freely soluble compound whose dissolution rate is controlled by tablet disintegration rather than by thermodynamic solubility, biorelevant media offer limited discriminating power — which is precisely the outcome observed.

3.6.2 Dapagliflozin — Micellar Acceleration

DAP profiles diverge markedly. FeSSIF-V2 released 55.47 ± 0.48% at 5 min and reached 85.84 ± 1.55% at 15 min — approximately 18 percentage points ahead of FaSSIF-V2 (73.26%) and 18–20 points ahead of compendial buffers at the same time point (Table 13). Micellar solubilisation is the mechanism: FeSSIF-V2 contains 10 mM sodium taurocholate and 2 mM lecithin, compared to 3 mM and 0.2 mM in FaSSIF-V2, and DAP partitioning into the micelle core scales with taurocholate concentration above the CMC (Mithani et al., 1996; Wiedmann et al., 2002). At logP 2.3, DAP sits within the solubility-enhancement zone identified for moderately lipophilic compounds by Galia et al. (1998). FaSSGF — low pH, minimal surfactant — produced the slowest profile (68.70% at 15 min), consistent with limited DAP aqueous solubility at pH 1.2 without bile-salt assistance. Pairwise f_2 values confirmed profile dissimilarity for DAP comparisons involving FeSSIF-V2 (f_2 = 45.84 for FeSSIF-V2 vs. pH 6.8; f_2 = 48.54 for FaSSIF-V2 vs. FeSSIF-V2), while all other DAP pairings were similar ($f_2 \geq 86$; Table 14) — a drug-specific discriminatory signal that compendial pH 6.8 buffer cannot detect.

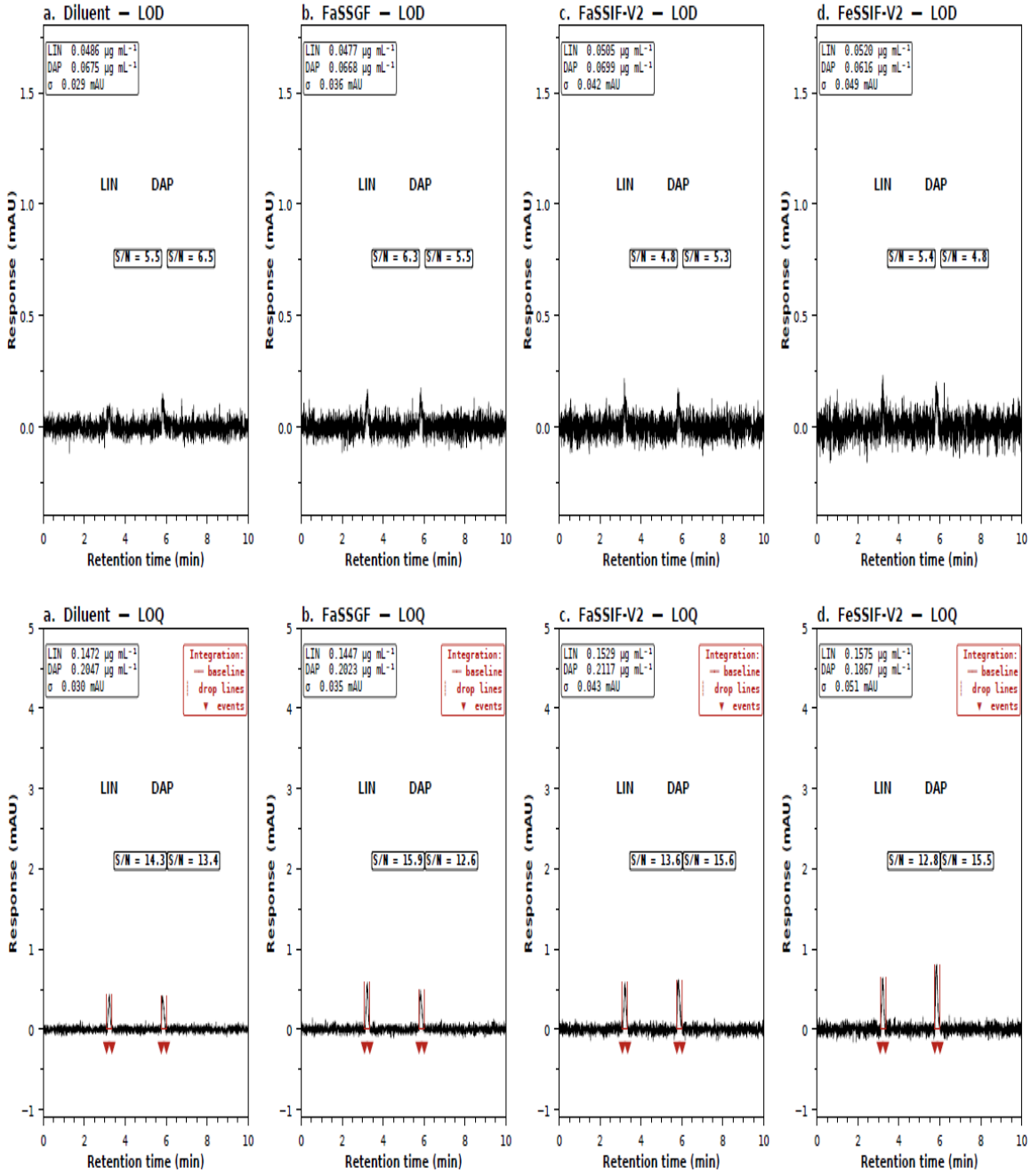

Figure 7: LOD and LOQ chromatograms of Linagliptin and Dapagliflozin in Diluent, FaSSGF, FaSSIF and FeSSIF conditions.

Table 13. Cumulative dissolution profiles (mean ± SD; n = 6 vessels) in six media

Drug	Medium	5 min	10 min	15 min	20 min	30 min	45 min	60 min
LIN	FaSSGF	41.79±0.62	66.92±1.59	79.18±2.37	86.75±1.59	93.34±1.03	96.28±1.96	99.06±0.57
LIN	FaSSIF-V2	38.98±1.21	62.13±1.06	76.40±1.76	85.40±2.24	91.98±1.89	94.22±2.63	96.91±1.51
LIN	FeSSIF-V2	34.67±0.96	58.63±1.12	72.81±1.76	82.66±1.07	91.79±1.87	94.57±1.06	96.70±2.22
LIN	0.1 N HCl	44.08±1.44	67.23±1.22	80.58±0.85	86.84±1.97	92.93±1.30	96.81±2.06	98.37±1.65
LIN	pH 4.5 Acetate	40.58±0.72	63.74±1.80	78.51±0.94	86.62±1.46	91.89±2.20	96.09±2.67	97.29±1.51
LIN	pH 6.8 Phosphate	38.73±0.66	62.57±0.86	75.43±2.45	85.59±1.86	92.62±1.55	96.30±1.73	96.84±2.27
DAP	FaSSGF	32.32±0.66	54.07±1.15	68.70±0.22	77.76±1.83	86.11±1.36	91.31±3.08	94.76±2.48
DAP	FaSSIF-V2	38.56±0.99	61.20±1.07	73.26±1.31	82.62±2.14	90.04±1.55	93.90±2.64	96.23±0.81
DAP	FeSSIF-V2	55.47±0.48	75.55±1.63	85.84±1.55	91.68±0.86	96.35±1.88	97.56±1.49	99.13±0.62
DAP	0.1 N HCl	30.49±0.80	51.98±1.18	67.42±1.50	77.31±1.36	84.98±0.94	89.42±1.91	92.78±1.09
DAP	pH 4.5 Acetate	33.71±0.60	55.63±0.54	71.23±0.95	80.14±0.79	87.47±1.85	93.23±1.04	95.15±1.59
DAP	pH 6.8 Phosphate	36.43±1.00	58.23±1.02	72.89±1.61	81.51±1.84	88.21±2.05	94.36±1.95	95.96±2.95

Values are % of label claim ± SD. USP Type II paddle, 900 mL, 37.0 ± 0.5 °C, 75 rpm (USP, 2023b; FDA, 1997).

3.7 Tablet Assay

Six independent assays of the DCGI-approved FDC tablet (Table 15) returned 99.997 ± 0.187% %RSD for LIN and 99.893 ± 0.183% %RSD for DAP — both within 98–102% of label claim, %RSD < 0.2%. Values are concordant with assay data reported for closely related LIN–DAP formulations by Shah and Kotadiya (2025) and Devda and Kotadiya (2025). Against those prior methods, the present work adds full ICH Q2(R1)/Q2(R2) validation in three biorelevant matrices and forced degradation inside those matrices.

Table 14. f_2 similarity factor — pairwise dissolution profile comparisons

Drug	Pairing	f_2	Interpretation (cutoff = 50)
LIN	FaSSGF vs. 0.1 N HCl	91.56	Similar
LIN	FaSSIF-V2 vs. pH 6.8 Phosphate	93.30	Similar
LIN	FeSSIF-V2 vs. pH 6.8 Phosphate	77.01	Similar
LIN	FaSSIF-V2 vs. FeSSIF-V2	76.96	Similar
DAP	FaSSGF vs. 0.1 N HCl	86.04	Similar
DAP	FaSSIF-V2 vs. pH 6.8 Phosphate	86.02	Similar
DAP	FeSSIF-V2 vs. pH 6.8 Phosphate	45.84	Dissimilar
DAP	FaSSIF-V2 vs. FeSSIF-V2	48.54	Dissimilar

f_2 calculated per Moore and Flanner (1996) as adopted by FDA (1997). Time points with mean release ≥ 85% excluded; minimum three qualifying points required.

Table 15. Tablet assay — six preparations of the DCGI-approved LIN 2.5 mg + DAP 5 mg FDC

Preparation	LIN (% label claim)	DAP (% label claim)	Note
1	99.84	99.62	—
2	100.18	99.94	—
3	99.92	100.12	—
4	100.24	99.78	—
5	99.74	100.04	—
6	100.06	99.86	—
Mean	99.997	99.893	Both within 98–102%
%RSD	0.187%	0.183%	Pass (≤ 2.0%)

Acceptance: 98.0–102.0% label claim; %RSD ≤ 2.0% (CDSCO, 2024; USP, 2023c; ICH, 2005).

3.8 Comparison with Published Methods

Three prior simultaneous RP-HPLC methods for LIN and DAP have been published (Shah & Kotadiya, 2025; Devda & Kotadiya, 2025; Patel & Patel, 2023), each validated in simple aqueous buffers without extension into biorelevant intestinal media. None investigated whether bile-salt micelles alter the apparent degradation kinetics of either API. The present method extends the validated analytical window to FaSSGF, FaSSIF-V2, and FeSSIF-V2 under full ICH Q2(R1)/Q2(R2) compliance and is the first to document micellar protection of DAP degradation under controlled stress conditions — a meaningful analytical and biopharmaceutical advance over existing methods for this drug pair.

4. CONCLUSION:

A stability-indicating RP-HPLC method for the simultaneous quantification of linagliptin and dapagliflozin has been developed, validated across four biorelevant matrices, and applied to dissolution profiling of the DCGI-approved FDC tablet. Operating isocratically at 45:55 ACN : OPA (pH 3.0) on Inertsil ODS-3 with 224 nm detection, the method resolves both analytes in under 10 min with Rs = 7.68 and satisfies all ICH Q2(R1)/Q2(R2) criteria across diluent, FaSSGF, FaSSIF-V2, and FeSSIF-V2. Tablet assay returned mean label-claim values within 0.1% for both analytes.

Two findings extend beyond routine analytical characterisation. Forced degradation inside FaSSIF-V2 and FeSSIF-V2 — an approach not previously applied to this drug pair — revealed concentration-dependent micellar attenuation of DAP degradation (1.8–3.5 percentage points in FeSSIF-V2) consistent with pseudo-phase kinetic shielding, while linagliptin showed no protection, as its logP of 0.4 precludes meaningful micellar incorporation. Critically, no new degradation pathways emerged in either bile-salt medium; the micelle shifted the rate, not the chemistry — meaning diluent-derived impurity profiles remain valid for predicting intestinal degradant identity. Biorelevant dissolution then revealed that FeSSIF-V2 is a discriminating medium for DAP, returning $f_2 < 50$ for fed-versus-fasted comparisons, a signal that compendial pH 6.8 buffer produces no indication of. The approach developed here generalises directly to other gliflozin-containing FDCs where micellar solubilization governs biopharmaceutical performance.

REFERENCES:

1. Bakshi, M., & Singh, S. (2002). Development of validated stability-indicating assay methods — Critical review. Journal of Pharmaceutical and Biomedical Analysis, 28(6), 1011–1040. https://doi.org/10.1016/S0731-7085(02)00047-
2. Bangalore, S., Kamalakkannan, G., Parkar, S., & Messerli, F. H. (2007). Fixed-dose combinations improve medication compliance: A meta-analysis. American Journal of Medicine, 120(8), 713–719. https://doi.org/10.1016/j.amjmed.2006.08.033
3. Blessy, M., Patel, R. D., Prajapati, P. N., & Agrawal, Y. K. (2014). Development of forced degradation and stability indicating studies of drugs — A review. Journal of Pharmaceutical Analysis, 4(3), 159–165. https://pmc.ncbi.nlm.nih.gov/articles/PMC5761119/
4. Central Drugs Standard Control Organization. (2024). List of fixed-dose combinations approved by DCG(I) — November 2024. https://cdsco.gov.in/
5. Devda, B., & Kotadiya, R. (2025). Stability-indicating RP-HPLC method for simultaneous quantification of linagliptin and dapagliflozin in fixed-dose combination. Separation Science Plus, 8. https://doi.org/10.1002/sscp.70162
6. Food and Drug Administration. (1997). Guidance for industry: Dissolution testing of immediate release solid oral dosage forms. https://www.fda.gov/
7. Food and Drug Administration. (2018). Dissolution testing and acceptance criteria for immediate-release solid oral dosage form drug products containing high solubility drug substances. https://www.fda.gov/media/115403/download
8. Fuchs, A., & Dressman, J. B. (2014). Composition and physicochemical properties of fasted-state human duodenal and jejunal fluids. Journal of Pharmaceutical Sciences, 103(11), 3398–3411. https://doi.org/10.1002/jps.24183
9. Galia, E., Nicolaides, E., Hörter, D., Löbenberg, R., Reppas, C., & Dressman, J. B. (1998). Evaluation of various dissolution media for predicting in vivo performance of class I and II drugs. Pharmaceutical Research, 15(5), 698–705. https://doi.org/10.1023/A:1011910801212
10. Graefe-Mody, U., Retlich, S., & Friedrich, C. (2012). Clinical pharmacokinetics and pharmacodynamics of linagliptin. Clinical Pharmacokinetics, 51(7), 411–427. https://doi.org/10.2165/11630900-000000000-00000
11. International Council for Harmonisation. (1996). ICH Q1B: Photostability testing of new drug substances and products. https://database.ich.org/

12. International Council for Harmonisation. (2003). ICH Q1A(R2): Stability testing of new drug substances and products. https://database.ich.org/
13. International Council for Harmonisation. (2005). ICH Q2(R1): Validation of analytical procedures. https://database.ich.org/
14. International Council for Harmonisation. (2023). ICH Q2(R2): Validation of analytical procedures. https://database.ich.org/
15. International Diabetes Federation. (2021). IDF Diabetes Atlas (10th ed.). https://www.diabetesatlas.org/
16. Jantratid, E., Janssen, N., Reppas, C., & Dressman, J. B. (2008). Dissolution media simulating conditions in the proximal human gastrointestinal tract: An update. Pharmaceutical Research, 25(7), 1663–1676. https://doi.org/10.1007/s11095-008-9569-4
17. Kasichayanula, S., Liu, X., Lacreta, F., Griffen, S. C., & Boulton, D. W. (2012). Clinical pharmacokinetics and pharmacodynamics of dapagliflozin. Clinical Pharmacokinetics, 51(6), 351–366. https://doi.org/10.2165/11631730-000000000-00000
18. Karthikeyan, K., & Vijayalakshmi, R. (2012). Investigations on filter compatibility for biorelevant dissolution sampling. International Journal of Pharma Sciences and Research, 3(6), 819–828.
19. K. Pavan Kumar and Amit Kumar. Modulation Of Beclin-1 and Bcl-2 Expression by Intermittent Fasting In CRC: Links to Autophagy and Apoptosis. International Journal of Pharmacy and Biological Sciences, 2025; 15(4): 91 115.
20. K. Pavan Kumar and Amit Kumar. Intermittent Fasting-Induced Autophagy and Apoptosis in Colorectal Carcinoma: The Role of Beclin-1 and Bcl-2. International Journal of Pharmaceutical Biological and Chemical Sciences, 2025; 14(4): 26-38.
21. Kokkula PavanKumar, Rajeev Imadi, Prasad Garrepally, S Nikitha Anthelmintic Activity of Some Medicinal Plants: A Short Review, International Journal of Pharmacy and Biological Sciences, 2019; 9(2): 605-611.
22. Kokkula Pavan Kumar, Ampati Srinivas and Prasad Garrepally, Hyperthermia has consistently improved the efficacy of radiotherapy and chemotherapy for many types of cancers, Journal of Stem cell Research and Therapeutics International, 2019; 1(003): 1-3.
23. Kokkula Pavan Kumar, Ampati Srinivas and Prasad Garrepally, Subcutaneous DL technique has proven to be an adequate host for human embryonic stem cells, Journal of Stem cell Research and Therapeutics International, 2019; 1(004): 1-3.
24. Kokkula Pavan Kumar, Boda Rambabu, Investigational studies on carcinoma in male SD rats, International Journal of Research and Analytical Reviews, 2019; 6(2): 654-662.
25. K. Pavan Kumar, G. Venkateshwarlu, Navaneeth Kumar, Mukesh Sharma, Rekha Pal, Taniya Rawat, E. Rajeswari, Wound healing activity of Indian Medicinal Plants, High Technology Letters, 2022; 28(2): 1-7.
26. K. Pavan Kumar, G. Venkateshwarlu, Mukesh Chandra Sharma, Govind pal, Rekha pal, Taniya Rawat, Invitro anthelmintic activity of alcoholic and methanolic extracts of seeds of Panicum miliaceum in Indian adult earthworm, High Technology Letters, 2022; 28(1): 800-809.
27. Maciel, F. M., Lourenço, F. R., & Pinto, T. de J. A. (2017). Development and validation of a dissolution test for dapagliflozin tablets. International Journal of Analytical Chemistry, 2017, Article 1521687. https://pmc.ncbi.nlm.nih.gov/articles/PMC5554998/
28. Markopoulos, C., Andreas, C. J., Vertzoni, M., Dressman, J., & Reppas, C. (2015). In-vitro simulation of luminal conditions for evaluation of performance of oral drug products. European Journal of Pharmaceutics and Biopharmaceutics, 93, 173–182. https://doi.org/10.1016/j.ejpb.2015.03.009
29. Matuszewski, B. K., Constanzer, M. L., & Chavez-Eng, C. M. (2003). Strategies for the assessment of matrix effect in quantitative bioanalytical methods based on HPLC-MS/MS. Analytical Chemistry, 75(13), 3019–3030. https://doi.org/10.1021/ac020361s
30. Mithani, S. D., Bakatselou, V., TenHoor, C. N., & Dressman, J. B. (1996). Estimation of the increase in solubility of drugs as a function of bile salt concentration. Pharmaceutical Research, 13(1), 163–167. https://doi.org/10.1023/A:1016062224568
31. Moore, J. W., & Flanner, H. H. (1996). Mathematical comparison of dissolution profiles. Pharmaceutical Technology, 20(6), 64–74.
32. Murugesan, A. (2022). RP-HPLC method development and validation for the estimation of dapagliflozin in bulk and dosage form. International Journal of Applied Pharmaceutics, 14(2), 142–148. https://doi.org/10.22159/ijap.2022v14i2.43482
33. Narayanan, L., Hari Krishnan, R., & Veerappan, M. (2017). Identification, isolation and characterization of major degradation product in

linagliptin API. Scientia Pharmaceutica, 85(3), Article 27. https://pmc.ncbi.nlm.nih.gov/articles/PMC5620513/
34. Neue, U. D. (1997). HPLC columns: Theory, technology, and practice. Wiley-VCH.
35. Patel, P. M., & Patel, R. (2023). RP-HPLC method development and validation for simultaneous estimation of linagliptin and dapagliflozin. International Journal of Pharmaceutical Sciences Review and Research, 81(2), 89–95.
36. Pillay, V., Choonara, Y. E., Tomar, L. K., Tyagi, C., & Kumar, P. (2018). Filter compatibility evaluation in biorelevant dissolution sampling. Dissolution Technologies, 25(2), 24–32.
37. Polli, J. E., & Jamil, M. (2022). The mechanism of drug solubilisation by bile salt and lecithin micelles in biorelevant media. European Journal of Pharmaceutical Sciences, 180, Article 106331. https://pmc.ncbi.nlm.nih.gov/articles/PMC9850292/
38. Reddy, B. V., & Reddy, K. V. R. (2015). Validated RP-HPLC-UV method for the determination of linagliptin in tablet dosage form. Asian Journal of Pharmaceutical Analysis, 5(1), 14–19.
39. Shah, B., & Kotadiya, R. (2025). RP-HPLC method development and validation for the simultaneous determination of linagliptin and dapagliflozin. BMC Chemistry, 19, Article 156. https://bmcchem.biomedcentral.com/articles/10.1186/s13065-025-01620-0
40. Sharma, R., Patel, K., & Vyas, S. (2024). Eco-friendly stability-indicating RP-HPLC method for simultaneous estimation of dapagliflozin and telmisartan. International Journal of Drug Delivery Technology, 16(10s), Article 73.
41. Singh, S., & Bakshi, M. (2000). Guidance on conduct of stress tests to determine inherent stability of drugs. Pharmaceutical Technology On-Line, 24, 1–14.
42. Singh, S., & Junwal, M. (2024). Pharmaceutical forced degradation (stress testing): A review. LinkedIn Pulse. https://www.linkedin.com/pulse/pharmaceutical-forced-degradation-stress-testing-review-singh-wjvbc
43. Snyder, L. R., Kirkland, J. J., & Dolan, J. W. (2010). Introduction to modern liquid chromatography (3rd ed.). Wiley. https://doi.org/10.1002/9780470508183
44. Sugano, K., & Takeru, F. (2023). Computational modelling of bile-salt micelle effects on drug solubility and permeability. ADMET and DMPK, 11(3), 357–376. https://pmc.ncbi.nlm.nih.gov/articles/PMC10567067/
45. United States Pharmacopeial Convention. (2023a). USP general chapter <621> Chromatography. In USP–NF. https://www.usp.org/
46. United States Pharmacopeial Convention. (2023b). USP general chapter <1092> The dissolution procedure. In USP–NF. https://www.usp.org/
47. United States Pharmacopeial Convention. (2023c). USP general chapter <711> Dissolution. In USP–NF. https://www.usp.org/
48. Vertzoni, M., Dressman, J., Butler, J., Hempen stall, J., & Reppas, C. (2005). Simulation of fasting gastric conditions and its importance for the in vivo dissolution of lipophilic compounds. European Journal of Pharmaceutics and Biopharmaceutics, 60(3), 413–417. https://doi.org/10.1016/j.ejpb.2005.03.002
49. White, W. B., Cannon, C. P., Heller, S. R., Nissen, S. E., Bergenstal, R. M., Bakris, G. L., & Jakubonienė, N. (2013). Alogliptin after acute coronary syndrome in patients with type 2 diabetes. New England Journal of Medicine, 369(14), 1327–1335. https://doi.org/10.1056/NEJMoa1305889
50. Wiedmann, T. S., Liang, W., & Kamel, L. (2002). Examination of the solubilization of drugs by bile salt micelles. Journal of Pharmaceutical Sciences, 91(8), 1743–1764. https://doi.org/10.1002/jps.10194
51. Wu, C.-Y., & Benet, L. Z. (2005). Predicting drug disposition via application of BCS. Pharmaceutical Research, 22(1), 11–23. https://doi.org/10.1007/s11095-004-9004-4
52. Zinman, B., Wanner, C., Lachin, J. M., Fitchett, D., Bluhmki, E., Hantel, S., Mattheus, M., Devins, T., Johansen, O. E., Woerle, H. J., Broedl, U. C., & Inzucchi, S. E. (2015). Empagliflozin, cardiovascular outcomes, and mortality in type 2 diabetes. New England Journal of Medicine, 373(22), 2117–2128. https://doi.org/10.1056/NEJMoa1504720